Toward Plasma-Assisted Ignition in Scramjets

Lance S. Jacobsen, Campbell D. Carter, Robert A. Baurle, and Thomas A. Jackson
Air Force Research Laboratory, WPAFB, Ohio

Abstract

The Air Force plasma ignition program is assessing the prospect of main-fuel ignition with plasma generating devices in a supersonic flow. As the study progresses, baseline conditions of operation are being established – such as, the required operational time of the device to initiate a combustion shock train. The two plasma torches currently under investigation consist of a DC constricted-arc design from the Virginia Polytechnic Institute and State University and an AC un-constricted-arc design based on a modified spark-plug from Polytechnic University. The plasma torches are realistic in size and operate within current power constraints while differing substantially in orifice geometry. In order to compare the potential of each concept, the flow physics of each part of the igniter/fuel-injector/combustor system are being studied. In each step of the program, we utilize CFD and experiments to help define and advance the ignition process. To understand the constraints involved with ignition process of a hydrocarbon fuel jet, an experimental effort to study gaseous and liquid hydrocarbons is underway, involving the testing of ethylene and JP-7 fuels with nitrogen and air plasmas. Results from the individual igniter studies have shown the plasma igniters to produce hot pockets of highly excited gas with peak temperatures up to (and in some cases above) 5000 K at only 2-kW total input power. In addition, ethylene and JP-7 flames with a significant level of OH, as determined by OH PLIF, were also produced in a Mach-2 supersonic flow with a total temperature and pressure of 590 K and 5.4 atm, respectively.

Introduction[1,2,3,4,5,6,7]

The scramjet engine has no low-speed propulsive capability; it must be boosted to high speed by another propulsion cycle. The scramjet can begin to function at approximately Mach 4. There is interest in the scramjet, both hydrogen and hydrocarbon fueled, for fuel-efficient high-speed flight and space access. Reliable, repeatable ignition of the scramjet at its Mach-4 take-over point is a persistent concern.

Report Documentation Page

Form Approved
OMB No. 0704-0188

Public reporting burden for the collection of information is estimated to average 1 hour per response, including the time for reviewing instructions, searching existing data sources, gathering and maintaining the data needed, and completing and reviewing the collection of information. Send comments regarding this burden estimate or any other aspect of this collection of information, including suggestions for reducing this burden, to Washington Headquarters Services, Directorate for Information Operations and Reports, 1215 Jefferson Davis Highway, Suite 1204, Arlington VA 22202-4302. Respondents should be aware that notwithstanding any other provision of law, no person shall be subject to a penalty for failing to comply with a collection of information if it does not display a currently valid OMB control number.

1. REPORT DATE	2. REPORT TYPE	3. DATES COVERED
20 OCT 2003	**N/A**	**-**

4. TITLE AND SUBTITLE	5a. CONTRACT NUMBER
Toward Plasma-Assisted Ignition in Scramjets	5b. GRANT NUMBER
	5c. PROGRAM ELEMENT NUMBER
6. AUTHOR(S)	5d. PROJECT NUMBER
	5e. TASK NUMBER
	5f. WORK UNIT NUMBER
7. PERFORMING ORGANIZATION NAME(S) AND ADDRESS(ES)	8. PERFORMING ORGANIZATION REPORT NUMBER
Air Force Research Laboratory, WPAFB, Ohio	
9. SPONSORING/MONITORING AGENCY NAME(S) AND ADDRESS(ES)	10. SPONSOR/MONITOR'S ACRONYM(S)
	11. SPONSOR/MONITOR'S REPORT NUMBER(S)

12. DISTRIBUTION/AVAILABILITY STATEMENT

Approved for public release, distribution unlimited

13. SUPPLEMENTARY NOTES

See also ADM001739, Thermochemical processes in plasma aerodynamics (Conference Proceedings, 28-31 July 2003 (CSP 03-5031)., The original document contains color images.

14. ABSTRACT

15. SUBJECT TERMS

16. SECURITY CLASSIFICATION OF:			17. LIMITATION OF ABSTRACT	18. NUMBER OF PAGES	19a. NAME OF RESPONSIBLE PERSON
a. REPORT	b. ABSTRACT	c. THIS PAGE			
unclassified	**unclassified**	**unclassified**	**UU**	**26**	

Ignition systems used to support ground-test research and development of the scramjet are not readily transferred to in-flight operation. In ground tests either an aerodynamic or physical restriction of the supersonic flow through the engine is applied to slow the flow through the combustor and raise the static pressure and temperature. This establishes a pre-combustion shock train in advance of the fuel-injection/flame-holding region. Sufficient heat release in the combustor makes this process self-sustaining, and the starting aid can then be removed. Alternatively a kinetic accelerant is used to aid the fuel-air mixture within the engine flow path to release sufficient heat to backpressure the combustion region. Again, if successful, the starting aid can be removed once combustion is achieved as the precombustion
shock is sustained through heat release.

The in-flight equivalent of these processes requires incorporation of storage, control, and delivery systems for a secondary supply of gas (aerodynamic blockage) or materials such as silane (accelerant). These ignition techniques are effective but increase system weight
and complexity and can introduce significant handling/safety issues. Even more onerous, however, is that the reliability and repeatability of these approaches may be inadequate, especially for a reusable system. The ignition process is a balance between blockage introduced for ignition, and that resulting from the heat released by fuel-air combustion. Too much backpressure will un-start the engine inlet; too little backpressure fails to achieve the selfsustaining condition. Finally, these approaches permit a small number of engine ignition attempts; and probably no re-start attempts.

Plasma-based ignition offers a technology alternative for adding large amounts of energy to specific regions of the scramjet flow-field. Duration and repetition of the applied power can be tailored to the ignition requirements. Power supplies can be developed to deliver enormous amounts of energy for short periods of time. Average power requirements, pulse duration and frequency, and spatial location are all within the designer's control. At issue is whether control over these parameters is sufficient to accelerate the fuel-air kinetic rates enough to achieve the self-sustaining condition within the scramjet flow-path at a Mach-4 flight condition.

This paper centers on the use of plasma to establish main-fuel ignition with sufficient heat release to form a precombustion shock, one of sufficient strength to make the combustion self-sustaining at Mach 4 flight conditions. Our premise is that torch placement relative to fuel injection sites is the critical parameter in a successful scramjet ignition attempt. Other important variables include the applied power and the plasma feedstock. The investigation
is both computational and experimental. In the discussion that follows the computational approach is outlined and initial results presented. The balance of the paper focuses on the torch technology

and the interaction of the torch and a fuel injector in a supersonic flow-field. Finally, experimental verification of the computation is described.

Background

Plasma ignition devices have been a topic of interest in the study of supersonic combustion for over twenty years.[1-7] The most common type investigated has been the arc discharge. Other types, including microwave and pre-arc streamers, have also been considered and are in development. The arc discharge device discussed in this paper is a plasma torch, in which the arc is coupled to a stream of gas. This device is compact and provides a source of hot, thermal energy with an abundance of excited and ionized species. Its configuration permits localized variation of position of the plasma jet along the walls of a combustor, which, with proper placement, could be used to ignite, hold, and potentially enhance combustion.[8]

Conditions inside the scramjet combustor do not favor autoignition at Mach 4 for either hydrogen or hydrocarbon fuel and do not necessarily get better with increasing flight Mach number. On a typical constant dynamic pressure trajectory, as the flight Mach number increases, the static temperature stays relatively constant (or gradually increases depending on inlet-combustor configuration) and the static pressure goes down. In addition, the air velocity increases so that where ignition must begin, in a recirculation zone or wake of a fuel jet; the air has a shorter residence time. Conversely, the temperature in these regions is higher.
Nevertheless, it may become necessary to introduce more physical flameholding mechanisms into the combustor to increase the static pressure, as will be shown in an example at the end of this section.

Fuel selection plays a significant role in the ignition process. Limited work has been published in this area, with the focus predominantly on hydrogen and light hydrocarbons. Near Mach-4 flight conditions, examples of the influence of engine fuel on ignitability are shown in Figure 1. This figure consists of experimental scramjet ignition data published by several different authors and consists of some of the works cited in Table 1. The data in this graph show reported minimum ignition powers required by plasma-torch igniters used to ignite hydrogen, ethylene, ethane, and methane fuels in various scramjet combustor configurations with freestream Mach numbers ranging from 1.8 to 2.5. Also shown on this figure (dashed line) is a typical value of combustor air total temperature at Mach-4 flight conditions (907 K), with a combustor Mach number of 2. Here, the Mach-4 flight combustor total temperature is based on output from the JHU/APL Ramjet Performance Analysis code, RJPA[16], for an altitude of 22 km with a dynamic pressure of 0.5 atm (1000 psf) and a combustor Mach number of 2.0.[17] Clearly there have been

successful plasma ignition experiments at Mach-4 flight conditions for scramjets combustors fueled by hydrogen and ethylene.

Table 1. Plasma-assisted ignition experiments

Authors	Combustor Inlet Cross-Dimensions *cm*	Step Height *mm*	Mach No.	P_t *atm*	P *atm*	T_t *K*	Eqiv. Ratio ϕ	Igniter Feedstock	Input Power *kW*	Downstream Configuration Order
Kimura et al.[1,†]	2.5 x 3.3	–	2.1, 2.7	9.2, 30	1	290, 450	~0.1, ~0.07	H_2,N_2, Ar	4.7[††,§§]	Fuel/Fuel/Torch/Fuel
Northam et al.[2,†,‡,§,¶]	8.9 x 3.8	3.8 x 2[#]	2[*]	8	1	590 - 1800	0.16-0.47	Ar + H_2	1.5 - 3.4[††,§§]	Step/Fuel/Torch/Fuel
Wagner et al.[3,†]	8.9 x 3.8	3.8 x 2[#]	2[*]	8	1	780 - 1560	0.28	Ar + H_2	0.5 - 2.6[‡‡,¶¶]	Fuel/Step/Torch Fuel
Sato et al.[9,†]	14.7 x 3.2	3.2 x 2[#]	2.5[*]	10	0.6	1000 -2500	0.1 - 0.8	O_2, N_2, Air, Ar + H_2	3.2[‡‡,§§]	Torch/Step/Fuel
Masuya et al.[10,†]	14.7 x 3.2	3.2 x 3[#]	2.5[*]	10	0.6	800 - 2500	0.4 - 0.8	O_2, Air	1 - 5.5[‡‡,§§]	a) Torch/Step/Fuel b) Fuel/Torch/Fuel/Fuel c) Fuel/Torch/Cavity w/Fuel
Tomioka et al.[11,†]	25 x 6.7	4.0 x 2[#], 2.0 x 1[#]	2.6, 4.1, 5.3[*]	9.3, 55, 100	0.45, 0.25, 0.09	890 - 2600	0.1 - 1.0	O_2	1 - 1.5 x 2[††,§§]	a) Fuel/Torch/Step b) Fuel/Torch/Cavity w/Fuel c) Fuel/Torch/Step+Strut
Masuya et al.[12,†]	3.0 x 3.0	–	1.8	1	0.17	290	0.013	O_2, N_2, N_2 +H_2	1.5 - 6[‡‡,§§]	Fuel/Fuel/Torch/Fuel
Kobayashi et al.[13,†]	14.7 x 3.2	3.2 x 2[#]	2.5[*]	10	0.6	800 - 2500	0.4	O_2, (H_2+O_2**)	1 - 5.5[††,§§], (1 - 45)[††,¶¶]	Torch/Step/Fuel
Shuzenji et al.[14,¶]	3.0 x 2.0	5 x 1[#]	2	3.8	0.5	400	0.16	Air	4 - 6[‡‡,¶¶]	Fuel/Torch/Torch/Step
Masuya et al.[15,†]	3.0 x 3.0	–	2.3	1	0.17	273	0 - ~0.009	He, N_2, N_2+H_2	1.5 - 6.3[‡‡,§§]	Torch Only

* H_2 + O_2 vitiated air, [†] H_2 Fuel, [‡] C_2H_4 Fuel, [§] C_3H_6 Fuel, [¶] CH_4 Fuel, [#] Number of combustor walls with steps.
** Used H_2+O_2 micro-burner as comparison to plasma torch, [††] Net power, [‡‡] Total power, [§§] Water cooled, [¶¶] Un-cooled

Before discussing the data presented in Figure 1, it is important to come up with a general definition for successful ignition in a supersonic combustor. Throughout the works cited in this document, the definition changes slightly, depending on the available experimental tools. In addition, the typical total temperatures required for ignition in a practical scramjet, in general, are below the autoignition limits of the combined fuel and combustor configuration. Typically ignition has been documented by visible plume emmission[2,3] the output from Pitot and total temperature probes1, wall pressure rise[2,3,14,17], and wall temperature rise[9,10,13]. The concept of global ignition must also be introduced, because, ultimately in all of the plasmatorch configurations involving nearby fuel, in general, there will always be some degree of fuel-air combustion directly around the plasma torch jet. Global ignition here is defined as ignition which propagates a flame throughout the length and intended area of the combustor and produces enough heat release to generate a shock train throughout the axial length of the combustor. This may be measured by a continual pressure or temperature rise throughout the length of the combustor. With this definition successful ignition

does not imply that there has been a sufficient level of heat release necessary to thermally choke a combustor duct, but rather enough to separate the wall boundary layer and sustain a shock train while propagating a flame throughout the combustor volume.

In an interesting example of local ignition, Masuya et al.[15] have demonstrated that it is possible to sustain a shock train in a small (3.0 x 3.0 cm) duct having no step (or cavity) at low pressure and temperature (see Table 1) by the use of a plasma torch with a partial hydrogen feedstock. In this set of experiments, the feedstock from the plasma torch was a 50/50 mixture of hydrogen and nitrogen (by volume) producing an overall combustor equivalence ratio of 0.009 with no other source of fuel. Combustion in this experiment was only reported in the vicinity near the plasma torch jet, and the flame was reportedly quenched due to the low temperature in the duct. Thus in this sense, global ignition has not been achieved here, though a sufficient level of heat release has been reached to create enough blockage to separate the boundary layer in the vicinity of the plasma jet and drive a shock train upstream of the plasma torch.

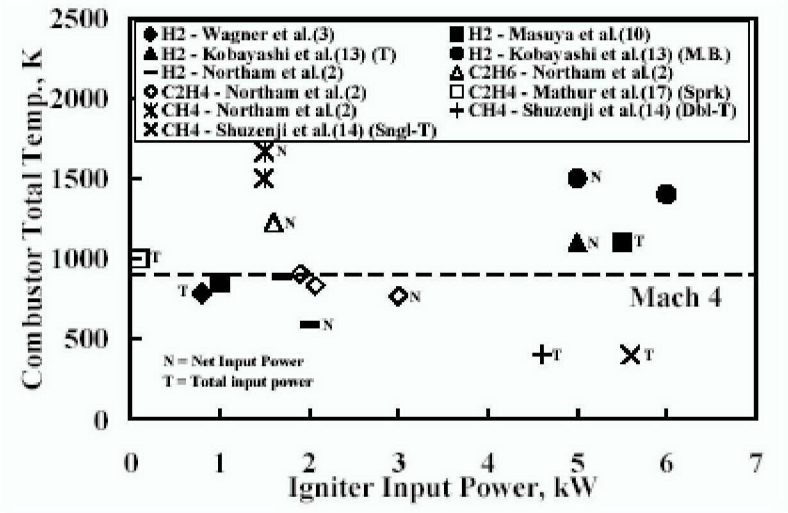

Figure 1. Global ignition in scramjets with different engine fuels

For the data presented by Northam et al.[2] with ethane and methane fuels (cross sectional dimensions of 8.9 x 3.8 cm), the minimum combustor total temperatures were far above the required level of 907 K (dashed line) for Mach-4 flight. However, ignition studies done by Shuzenji et al. [14] in a small supersonic test section with methane fuel injection (cross sectional dimensions of 3.0 x 2.0 cm with a 0.5 cm backwards facing step) have also been successful at very low total temperature (400 K). As to the success with Shuzenji's experiment, it is important to realize that this experiment used a very small combustor with no divergence in the test section and fairly high levels of input power in comparison to the larger, more realistic scramjet configuration used in Northam et al. [2] To date no experimental work has been published involving the successful ignition

of liquid hydrocarbon fuels without the use of a downstream back pressure generating device (aerothrottle).

Other points of interest in Figure 1 are the $H_2 + O_2$ micro burner (M.B.) used by Kobayashi et al.[13] and the double torch configuration (Dbl-T) shown by Shuzenji et al. [14] In both of these studies, the performance of the two devices was compared to that using single plasma-torch igniters. Masuya et al. [10] have also examined the influence of cross-stream duct placement on the ignitability of a scramjet combustor. In this study it was found that by placement of a plasma torch on the small length of their combustor (14.7 x 3.2-cm cross-dimensions) and by adding a step to this small length, they significantly reduced the input power required to ignite the engine while considerably reducing the required total temperature as well.

Scramjet combustors are typically designed with emphasis on flameholding and efficient combustion. Usually ignition concepts are then integrated into the engines afterward so that the problem becomes one of how to ignite the particular combustor. Along these lines, it may be beneficial to alter particular aspects of proven combustor geometry, such as the location of fuel relative to flameholding mechanisms, or additional subsonic areas to allow sufficient heat release necessary to initiate and propagate main fuel combustion. The point here is that a design with adequate flameholding may be inadequate for particular ignition strategies.

To obtain a better understanding of the differences between sufficient conditions for flameholding and ignition, it is useful to examine the work done by Mathur et al.[17] In this study, combustion experiments were performed in a uncooled combustor of rectangular cross section with four low-angled ethylene-fueled injectors arranged in a cross stream row, just upstream of a cavity flame holder. The cavity flame holder was lit with a spark plug and intense combustion was achieved over a wide range of equivalence ratios at a combustor total temperature of 1000 K. In one test case in their study, after main combustion was achieved, the total temperature was reduced to 944 K and vigorous combustion was maintained. During another test with this configuration, an attempt to start the combustor at 944 K was made over a wide range of fuel pressure with no success. According to Mathur et al.[17], the apparent hysteresis suggests that operation at lower stagnation temperatures is possible if the ethylene were heated. Clearly, the combustor conditions were not sufficient to produce the combustion shock train, and the flame from the cavity could not propagate into main duct. This implies that there must be a required level of energy, be it from heating the fuel or the freestream, to speed the heat release from ombustion of the main fuel jets thereby initiating a shock train.

Relevant to this work, a plasma-torch igniter offers another way to add the requisite energy. The ethylene-fuel (C_2H_4) ignition data presented in Figure 1 by Northam et al.[2] (step+plasma torch)

and Mathur et al.[17] (cavity+sparkplug) shows that it is possible to reduce the required total temperature needed to initiate combustion with a plasma torch past the cavity sparkplug configuration, from 1000 K to 767 K for 3 kW of net input power in a backward facing step flameholding configuration. Granted, this is not a direct comparison, since the two combustors had different geometries and used different forms of vitiated freestream air (JP-4 or $H_2 + O_2$); however, it does show that there is a potential to lower the freestream (combustor entrance) total temperature required for ignition by the use of one or more plasma torches. In addition, by careful placement, the plasma torch, by virtue of its jet momentum, can also be used to bridge the gap between a cavity flame and fuel jet, perhaps enhancing the flame-spreading process during ignition.

An example of the influence of flight Mach number and combustor geometry on a plasma-assisted ignition system is shown in Tomioka et al.[11] In this study Tomioka tested a complete scramjet engine in a free-jet facility, simulating flight Mach numbers of 4, 6, and 8. These tests involved freestream air heated with a storage heater at the Mach-4 and 6 conditions and air heated with a hydrogen/oxygen vitiator at the Mach-8 condition. The combustion tests involved hydrogen fuel injection in the scramjet engine, and the configuration included a step that was directly connected to additional steps on the sidewalls of the combustor, which helped to spread the flame around most of the combustor surface. Two oxygen plasma-torch igniters, each at 1 - 1.5 kW of net input power, were used to ignite the combustor. It was found that the original configuration, in which the two plasma torches were placed on the top wall 20-mm upstream of a backward facing step, was sufficient to ignite the flow only at Mach 4. To attain ignition at the Mach-6 condition, a cavity was incorporated into the region from the top wall step (making it deeper) to 40-mm downstream, and then oxygen was injected into the step region. This configuration provided only limited ignition, and the flame did not spread laterally throughout the combustor. Global ignition of the main fuel flow with this configuration was only possible when the main fuel flow rate was increased to a high level, which consequently increased the pressure in the base of the step region, allowing for more vigorous combustion. This meant that the ignition condition was restricted to a small range of combustor equivalence ratios. At this point to ensure a wide operational range for their scramjet, a short strut was added into the combustor – mounted from the center of the top combustor wall – with a height one-fifth of the engine. This strut was introduced with the sole purpose of increasing the pressure in the base of the flameholding steps (the cavity recess on the top wall and the auxiliary oxygen injector were removed from this configuration). This configuration successfully widened the operational fuelling range of the combustor at the Mach-6 condition. However, the pressure in the step regions was still not sufficiently high to ignite the engine at Mach 8.

Modeling the Ignition Process

The use of CFD is of paramount importance to aid in the establishment of program guidelines and to simplify the process of igniter placement in a scramjet combustor. Furthermore, the combined experimental-computational program allows interaction through each step of the program. Starting with the individual igniter evaluation, these experiments help validate the models used to simulate the plasma discharge. This, in turn, improves the confidence in the computational effort when the fuel and igniter are combined. Furthermore, calibration of the CFD routines with the combined flow experiments will help reduce and guide the overall experimental test matrix required with each igniter concept.

One insightful example of how CFD has been used to define the ignition problem in relation to the use of plasma torches in a full engine configuration is shown in the following calculations performed with the VULCAN[18] (Viscous Upwind aLgorithm for Complex flow ANalysis) software package. This routine solves the Reynoldsaveraged conservation equations for mixtures of thermally perfect gases using a cell-centered finite volume scheme.

Furthermore, the low diffusion flux split scheme (LDFSS) of Edwards[19] was used. A time-accurate integration was required once the plasma torches were activated to assess the ignition characteristics. The simulations were performed using an implicit dual time-stepping algorithm that combines a diagonalized approximate factorization scheme to integrate in pseudo-time, with a 3-point backwards finitedifference approximation for integration in real-time. This scheme provides the desired second-order temporal-accuracy without a stringent time-step restriction based on numerical stability. All time-accurate simulations were performed with a constant time-step of 0.1 microseconds.

The geometry of the injectors, cavity, and plasma torches simulated in this study are shown in Figure 2. A schematic of the combustor rig flowpath considered in this investigation is shown in Figure 3. The modeling assumptions for the plasma fluid employed in the CFD simulations neglect many important effects (MHD, ionization, etc.) that are likely to enhance the ability of the plasma to ignite the flow. In this study, the decision was made to ignite the flow within the cavity flameholder prior to the initiation of plasma into the system. This would provide a relatively large pool of hot combustion products, including radicals, to aid the plasma torches in igniting the flow. The calculations used a 10 reaction, 10 step mechanism to simulate ethylene combustion in air. [20] The plasma-torch plume was simulated by boundary conditions modeling 3.18 and 1.59-diameter holes with equilibrium air consisting of O_2, O, and N_2 and a uniform 3400 K temperature distribution, simulating 10 and 2.5 kW of net input power, for the two hole sizes, respectively. It is

interesting to note that both set of plasma-torch boundary conditions produced similar computational results.

The time history of the scramjet ignition process is shown in Figure 4 in the form of temperature contours. The elapsed time between each image is 0.3 ms. After 0.3 ms the lower portion of the fuel plume is starting to ignite. The combustion is somewhat more intense near the combustor sidewall, but overall the ignition process is relatively uniform over the entire combustor span. At 0.6 ms the flame has spread around the periphery of the fuel plumes, and the heat release is forcing the combusting fluid towards the cowl-side surface (opposite of the cavity side). At t = 0.9 and 1.2 ms, the combustion front has expanded to fill the entire cross-sectional area of the combustor just downstream of the cavity flameholder. The flame structure at this point is still relatively symmetric. The influence of the precombustion shock train that has formed due to the heat release of combustion is clearly seen at t = 1.5 and 1.8 ms. At this time, the combustion front has moved upstream of the fuel injection ports due to flow recirculation caused by shock/boundary-layer interactions. The pre-combustion shock train has also caused an asymmetry to develop near the sidewall/body-side juncture. This corner region has a relatively large volume of low-momentum flow, which tends to separate more readily than the thinner attached boundary layer that exists on the remaining sections of the combustor surface.

Despite the utility of CFD to assess the ignition process, the current computational methods are still too limited to rely upon as a sole method of analysis. Due to the necessity of reduced kinetics, simplified equations of motion, and the approximation of turbulence modeling in today's computational analysis, CFD currently is used as a guideline to help develop experimental directions and refine experimental matrices.

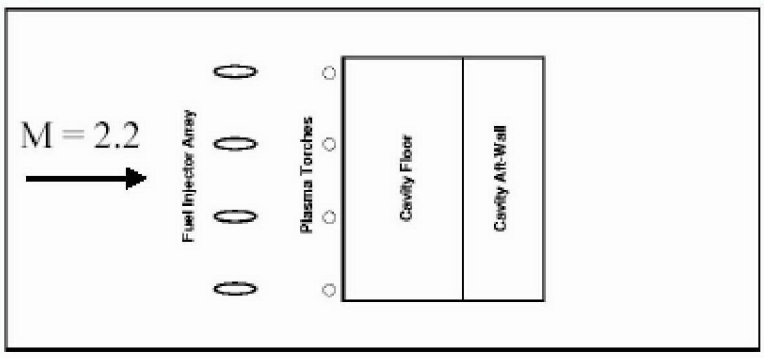

Figure 2. Injector/cavity configuration with simulated plasma torches.

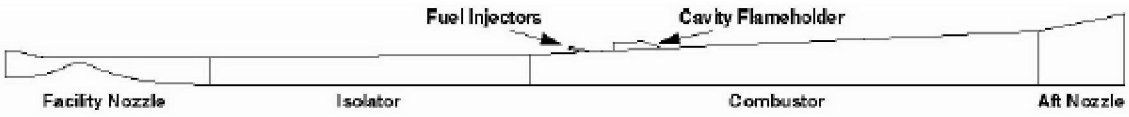

Figure 3. Simulated scramjet combustor flowpath.

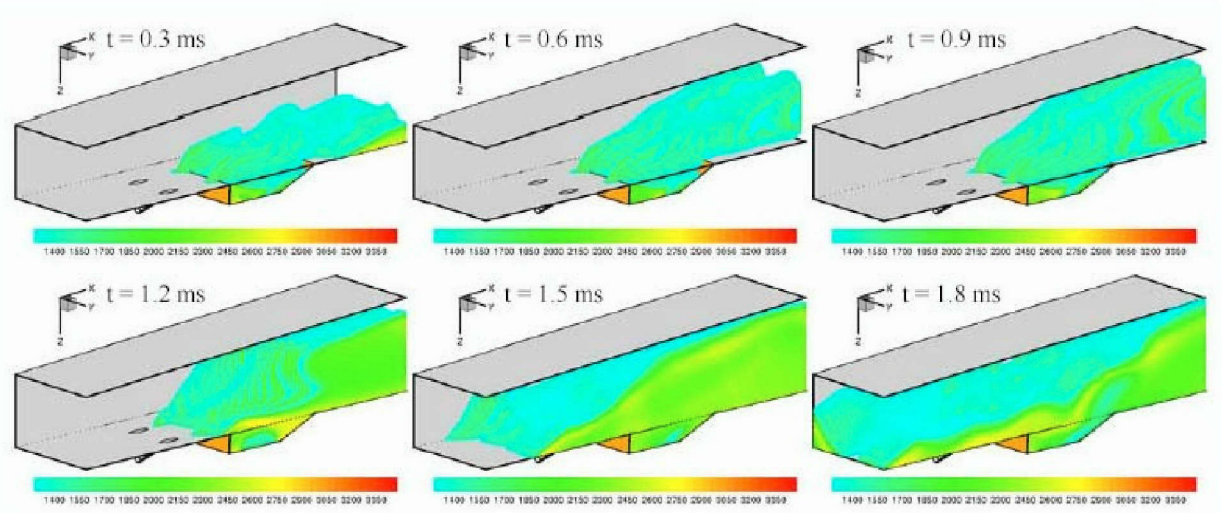

Figure 4. Temperature contours (K) describing the ignition process in a scramjet combustor (Evolving in time steps of 0.3 ms, from left to right starting at the top left corner).

Plasma-Torch Igniters

The two plasma torches currently under investigation consist of a DC constricted-arc design from Virginia Polytechnic Institute and State University21 and an AC unconstricted-arc design based on a modified spark-plug from Polytechnic University22. Both igniters are in the initial phase of the research effort. Prototypes have been built, and evaluation of their general characteristics and power utilization has begun. Each igniter being studied has been evaluated to some extent in a quiescent ambient environment. The primary objective here is to understand the operational and physical characteristics involved with each design. Once the flow-physics of a design are understood, advantages, disadvantages, and operational modes of interest can be established.

Design

Figures 5 and 6 show drawings of the Virginia Tech DC plasma torch and its two anode geometries being studied at present[21]. The VT plasma torch design consists of a constricted arc with a 1.59-mm throat diameter, d_t. Figure 7 shows a drawing of the Polytechnic University AC plasma torch with a 6.4-mm outer jet exit diameter and its feedstock plenum design for insertion into a supersonic facility discussed later in the paper. Both torches use a central

tungsten electrode. This piece functions as the cathode in the VT torch and alternates as both anode and cathode in the PU design. The VT torch is designed for flowrates ranging from 10 to 80 SLPM (standard liters per minute, reference to STP, such that, for example, 40 SLPM of N_2 equals 0.83 gm/sec) of air or nitrogen while the PU design can be operated from 0 to 1500 SLPM, the feedstock exit being choked at roughly 500~600 SLPM depending on the back pressure of the environment.

Figure 8 shows a graph of the steady-state thermal efficiency of the VT plasma torch, which typically has values of 90 percent or higher. Due to the nature of operation of the PU design, for example that its arc runs past the physical body of the torch (and is enveloped in the torch feedstock), the thermal efficiency of this design is also expected to be near unity.

Flow Characteristics

Figure 9 shows schlieren images taken with the (a) Virginia Tech DC and (b) Polytechnic University AC plasma-torch igniters, both with nitrogen feedstocks in a quiescent, ambient environment. The schlieren images were taken with a high-speed camera capable of recording 32 images at rates up to 1 million frames per second. The images show some of the differences associated with the two plasma torches in operation. With both torches an arc can be seen to emerge from the torch exit, penetrate vertically further into the plasma jet, bend 180 degrees around and land on the outside surface of the anode section. However, due to the differences in the configurations of the two torches involving flow rates, injector exit diameters, and voltage-current operational characteristics, the two flowfields show very different behavior: a narrow, constant jet in the VT design and a wide, pulsating jet in the PU design with a flow rate range one order of magnitude higher than with the VT design.

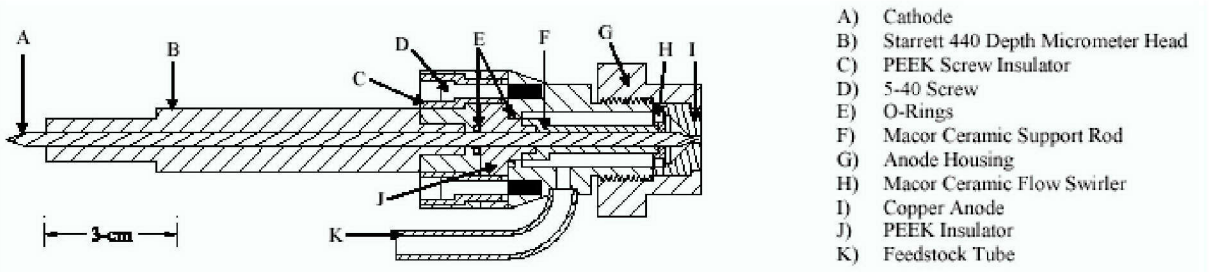

Figure 5 Virginia Polytechnic Institute and State University DC plasma-torch igniter.

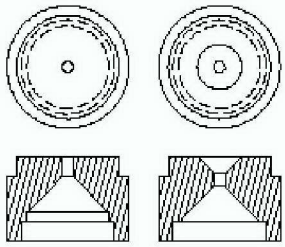

Figure 6. VT Plasma-torch anodes with 0-deg, sonic (left) and 45-deg, divergent constrictor angle (right).

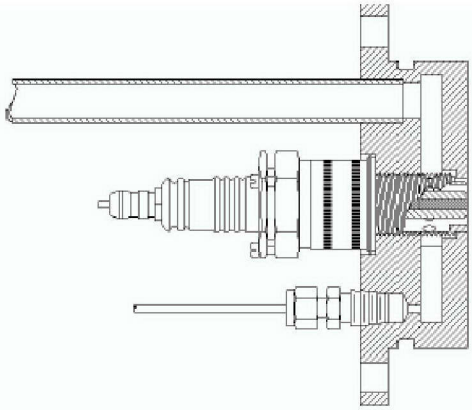

Figure 7. Polytechnic University AC plasma-torch igniter.

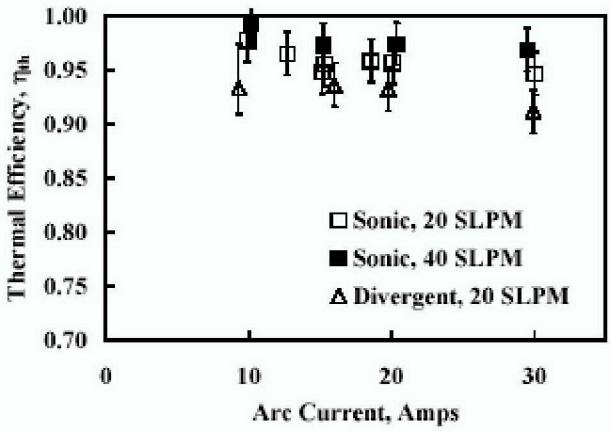

Figure 8. Plasma-torch thermal efficiency as a function of arc current.

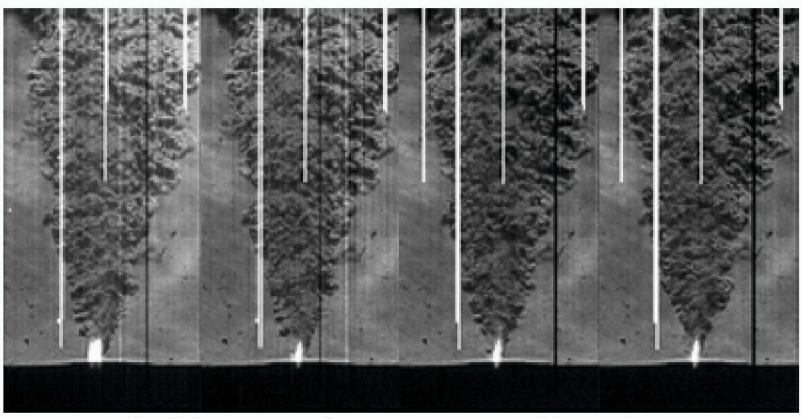

a) Virginia Tech DC plasma torch with sonic anode
(Interframe times = 0.1, 0.2, 0.4 milliseconds, left to right)

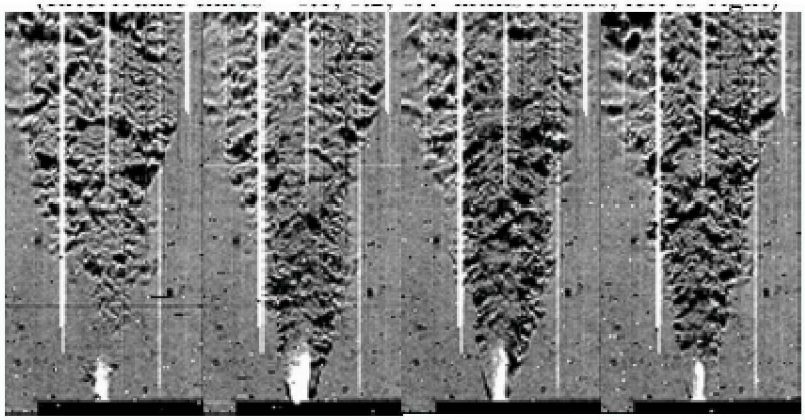

b) Polytechnic University AC plasma torch (Interframe time = 2 milliseconds)

Figure 9. Schlieren images of Virginia Tech and Polytechnic University plasma-torch igniters. (image size 9.9 X 5.0 cm).

The PU torch arc-voltage characteristics provide an arc with a voltage on the order of 400 volts at its peak power in the cycle, which for an equivalent power to the VT torch, produces an arc length about 4 times as long for a quarter of the required current. One further note of interest regarding behavior of the PU AC torch is that for the estimated ignition period of about 2 milliseconds, the torch is really behaving like a DC torch in that each pulse in its AC cycle is $1/120^{th}$ of a second long (~8 ms) so that the peak power portion of each pulse, on the order of 2 ms, is comparable to the required time necessary for the ignition process in a scramjet.

The time scales in the two sets of selected images were chosen as follows: for the VT torch, 0.1, 0.2, and 0.4-ms inter-frame times (from left to right) while for the PU torch, equal 2-ms inter-frame times. The variable inter-frame times of the VT torch allows one to observe the structures in the region near the arc and to obtain an understanding of the dynamics between the motion of the arc and the reaction of the plasma jet plume. The 2-ms inter-frame time for the PU torch shows the characteristics of a single pulse in its AC power cycle.

In Figure 10 results are shown from nitric oxide Planar Laser-Induced Fluorescence (NO PLIF) experiments with the VT plasma torch in operation with a nitrogen feedstock (40 SLPM) at total input power levels of 1 and 2 kW. These instantaneous images illustrate the various levels of NO concentration ranging from blue (Low) to red (High). Note that the image scales are each set to display the full range of individual flow features. In addition, the NO images have not been corrected for the effects of electronic quenching, Boltzmann fraction, or laser sheet non-uniformity. The hoop structure of the arc is especially clear in these images, and in both, the arc exits the plasma torch sonic orifice on the left side of the arc hoop and impacts on the torch anode to the right. A laminar region to the right of the hoop marks the region where the ambient air in the test

section is being entrained into the plasma jet and reacts with the plasma jet to form NO. A transition to turbulence can be seen at the top of the laminar structure, marked by the unsteady, highsignal-intensity NO region. Two regions of high NO level are shown at the centerline of the images and to the right in the above-mentioned entrainment region. It is interesting to note that the NO profiles, in a steady-state sense, reach a near symmetric state past about 11 torch throat diameters, d_t, downstream of the torch exit.

An instantaneous image pair of NO PLIF and temperature via Filtered Rayleigh Scattering (FRS) thermometry is shown in Figure 11. Both the NO PLIF and FRS temperature images are scaled to the maximum NO signal and temperature, respectively. The black colored portion of the image corresponds to emission from the plasma arc (that was not suppressed sufficiently through camera-intensifier gating and the interference filter). The rough outline of the NO profile from the first image in Figure 11 is overlaid on top of the second, temperature image. This was done to indicate the relationship between the hot temperature pockets created by the arc heating process and the formation of NO by the entrainment of air into the nitrogen plume. In some locations particle scattering (that "bleeds" through the filter) causes an erroneously low temperature; these particles originate from the electrodes near the arc attachment points. In the data reduction process, areas with particle scattering or arc emission were set to zero Kelvin by the use of a threshold filter and are visible as small white specs surrounded by regions of higher temperature in the FRS temperature image.

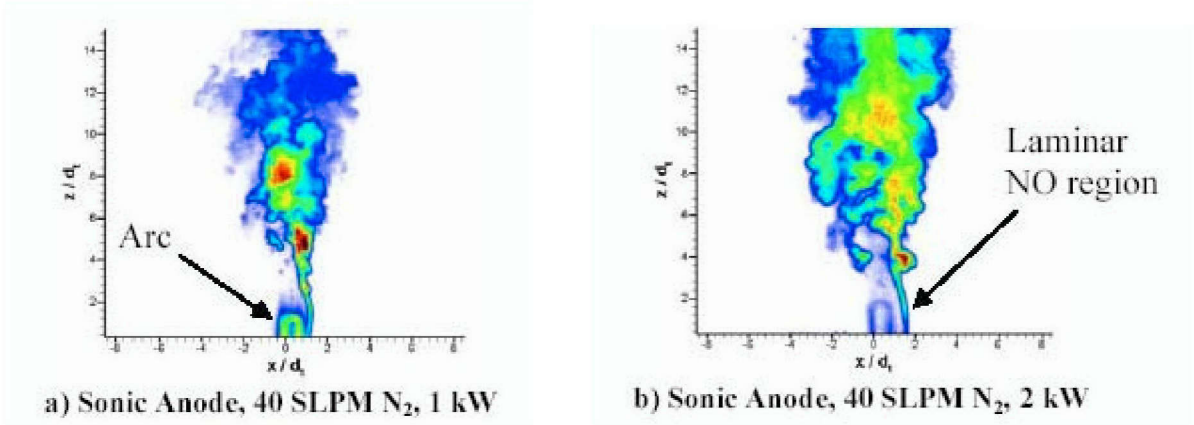

a) Sonic Anode, 40 SLPM N_2, 1 kW

b) Sonic Anode, 40 SLPM N_2, 2 kW

Figure 10. Instantaneous NO PLIF images of VT plasma torch in an ambient environment.

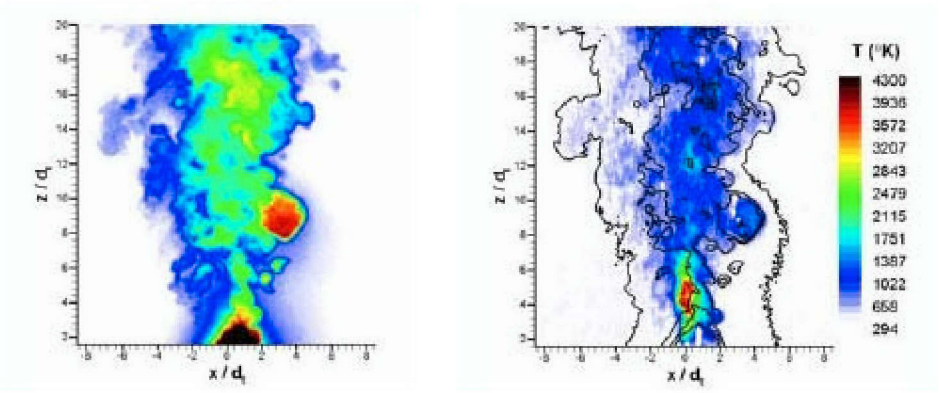

Figure 11. Simultaneous and instantaneous NO (top) and temperature (bottom) measurements with superimposed NO field (VT plasma torch with a divergent anode, 20 SLPM N_2, 2 kW).

In Behbahani et al.[23] the hot pockets of gas seen here were postulated to be from the thermal stratification of the plasma jet causing the arc to heat only a small portion of the plasma jet to exceedingly high temperatures. In these images, it is evident that the locations of high NO signal correspond well to the temperature region between 900 and 1300 K. The maximum temperature of the hot pockets shown in the two instantaneous profiles is indicative of the range of temperature in the plasma torch flow-field. For the 2-kW total input power level, maximum temperatures in the instantaneous images were above 5000 K. Due to the strong temperature-dependence of the Zeldovich NO production mechanism, the regions for NO production will strongly favor the highest temperature regions; however, these regions also have small O_2 concentration (since the O_2 originates from the surrounding air). Thus, the high-signal regions seen in the images reflect a complex mixing and production process.

Torch/Fuel Injector Interaction: Experiment

Critical to the success of plasma-assisted ignition will be the interaction of torch and fuel injector. At the most basic level, the torches under investigation exhibit insufficient momentum to significantly penetrate into the supersonic core flow characteristic of the scramjet. The momentum of the fuel plume, however, can be used to transport plasma to the fuel plume core to influence more of the reactants. Following full characterization of each torch, the evaluation shifts to combined fuel and igniter testing in supersonic flows.

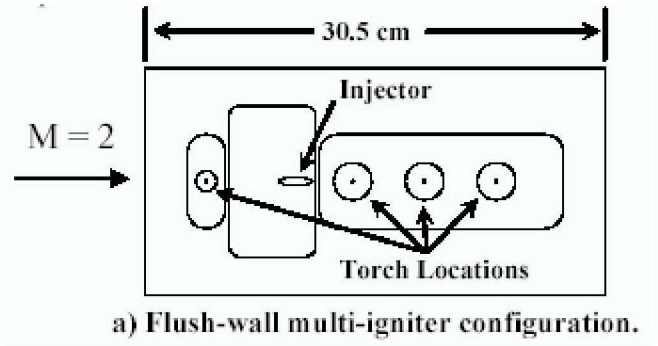

a) Flush-wall multi-igniter configuration.

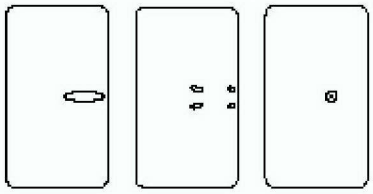

b) Fuel-injector inserts. From left to right: Single 15-deg hole, Aero-ramp, Barbotage.

Figure 12. Test hardware for cold-warm flow combined fuel and igniter experiments without a cavity based flame-holding system.

Initial evaluation is conducted in a supersonic, Mach-2 flow facility capable of heating the air to about 750 K. This facility allows testing of an individual concept with both gaseous and liquid hydrocarbon fuels without a cavity based flame-holder. A sketch of the plasma-torch and flush-wall injector inserts used in this study is shown in Figure 12. This 15.2 x 30.5 cm test section floor plate fits into a simulated scramjet combustor duct with an initial duct height of 5.1 cm. At the upstream edge of the test section insert, the simulated combustor section diverges on the injector side by 2.5 degrees. Total input power is reported. This particular hardware was intentionally designed not to study global ignition, per se (as indicated by a pressure rise), but to reduce the chance of causing global ignition by limiting the equivalence ratio of the tunnel below 0.1.

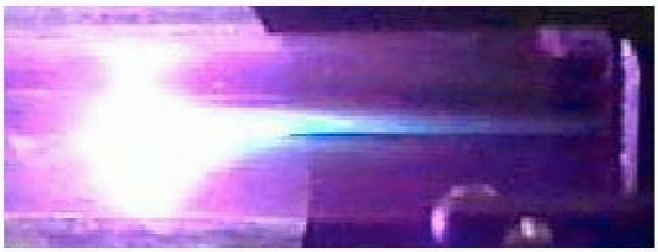

a) Single Hole (5.3 gm/sec, 318 K), Freestream (5.4 atm, 586K), PU Plasma Torch (5 KW Peak, 470 SLPM Air).

b) Aero-Ramp (5.4 gm/sec, 352 K), Freestream (5.4 atm, 592K), PU Plasma Torch (5 KW Peak, 470 SLPM Air).

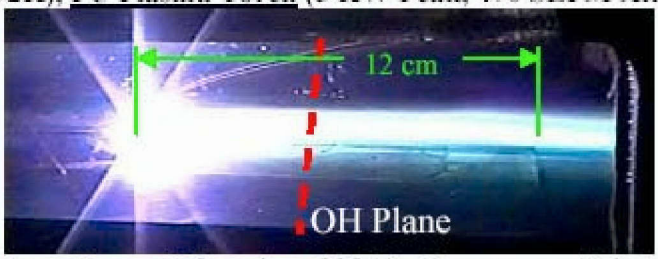

c) Aero-Ramp (5.2 gm/sec, 320 K), Freestream (5.4 atm, 588K), VT Plasma Torch (4 KW DC, 40 SLPM Air).

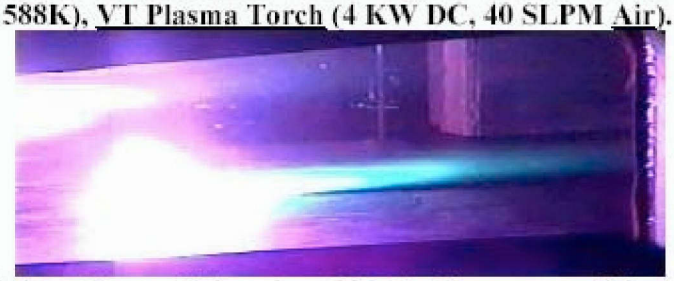

d) Aero-Ramp (5.4 gm/sec, 336 K), Freestream (5.4 atm, 586 K), VT Plasma Torch (4 KW DC, 40 SLPM N_2).

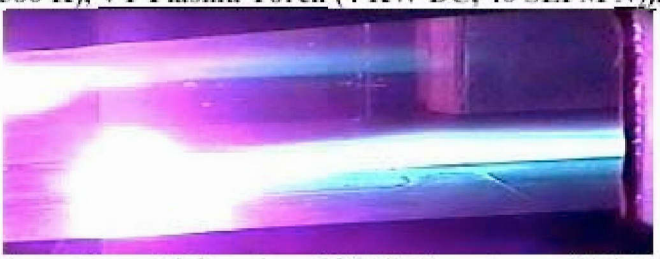

e) Aero-Ramp (3.3 gm/sec, 336 K), Freestream (5.4 atm, 586 K), VT Plasma Torch (4 KW DC, 40 SLPM N_2).

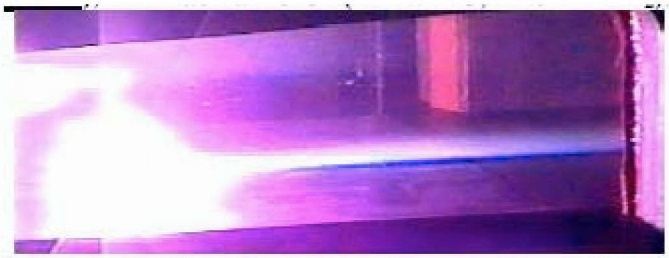

f) Aero-Ramp (3.4 gm/sec, 296 K), Freestream (5.4 atm, 305K), VT Plasma Torch (4 KW DC, 40 SLPM N_2).

Figure 13. Video image of the PU and VT plasma torches with an ethylene fueled aero-ramp injector upstream (not in view) in a Mach 2 flow. Flow is left to right, 12 cm from torch to downstream edge of insert.

In particular, this was accomplished by placing the fuel injector at the centerline of the tunnel and not adding any flame-holding mechanisms such as a cavity or backwardsfacing step. By doing this one can study the interactions of the fuel plume with the plasma torch by itself, and any flame produced is strictly created by this interaction (hence detaching the ignition and flameholding problems as much as possible from the combustor geometry).

Tests have been conducted using gaseous ethylene fuel with the 15-deg downstream-angled single-hole and aeroramp injectors similar in design to Jacobsen et al.[24] The barbotage aerated injector was also employed using room temperature, liquid JP-7 and nitrogen gas. At this point both igniters have been evaluated and injector/torch combinations have been identified which produce a substantial flame plume (both from flame chemiluminescence and OH PLIF). This is illustrated in Figure 13, which shows still shots from video recordings of the PU (a and b) and VT (c – f) plasma torches (sonic anode) in operation downstream (2nd downstream station) of the ethylene-fueled single-hole injector (a) and aeroramp injector (b – f). Each image is sequentially arranged so that only one parameter is different from one image to the next. The parameters of change are as follows: (a) single hole – (b) aero-ramp, (b) PU plasma torch – (c) VT plasma torch, (c) air feedstock – (d) N_2 feedstock, (d) 5.4 gm/sec – (e) 3.3 gm/sec, (e) 586 K freestream total temperature – (f) 305 K freestream total temperature.

The most noticeable features shown in this image sequence are that the VT torch produced a larger flame than the PU torch, in its current form (images b and c), for the same fuel and near power conditions. Several feedstock flowrates were tried with the PU torch over its operational range (0 – 1500 SLPM air) and a flowrate of ~500 SLPM air was determined to produce the longest visible flame for its current electrode configuration. Air was also determined to produce a longer flame when compared to Nitrogen as the torch feedstock with the VT torch (images c and d). This difference in flame size from images c and d indicates that this type of flame is very sensitive to the

local equivalence ratio and coupling of the ignition source with the mixture. In general with the VT torch, as the fuel flowrate was reduced, the flame length grew (images d and e) and propagated down the length of the combustor. When the freestream temperature was reduced, the flame diminished in intensity, though it is interesting to note that the length of the flame was still substantial (images e and f). A general comparison of the single-hole and the aero-ramp injectors (images a and b) is also shown, though to date an insufficient number of tests have been conducted with the single-hole injector to assess its performance relative to that of the aero-ramp.

Cross-stream OH PLIF images were generated for each torch station studied, 5-cm downstream of each plasma torch as noted by the red dashed line on the video still image (Figure 13C). The frame averaged OH PLIF false color images are shown in Figure 14. These OH images correspond to the test configurations with the aero-ramp injector and the first and second downstream plasma-torch stations. In either case, the maximum signal corresponds to red in the color table (though the signal levels are quite different). The field of view is 12 x 12 torch throat diameters, d_t, (1.9 x 1.9 cm) for both images. The data presented were taken at a nominal freestream total temperature of 590 K and total pressure of 5.4 atm with a fuel mass flow rate of ~ 5.3 gm/sec (ethylene). In both averaged images, the laser sheet was positioned 5.1-cm downstream of the exit of the center of the plasma torch orifices, corresponding to 8.9 and 13.7-cm downstream from the center of area of the aero-ramp injector, for stations 1 and 2, respectively. These data were presented to show the increase in penetration of the flame plume created by placing the plasma torch closer to the aero-ramp fuelinjector; here, the plasma jet is enveloped into the fuelplume counter-rotating axial-vortex pair. In general the dimensions of the overall fuel-plume were larger than the indicated in the images; rather, the flame plume was formed between two distinct fuel-jet cores.

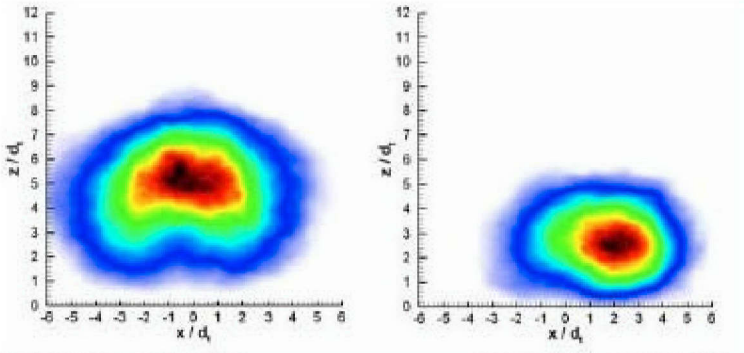

a) Torch-station #1 b) Torch-station #2

Figure 14. OH PLIF plumes with aero-ramp injector and VT plasma-torch igniter with an air feedstock. Laser sheet positioned 5.1 cm downstream of each relative downstream torch station.

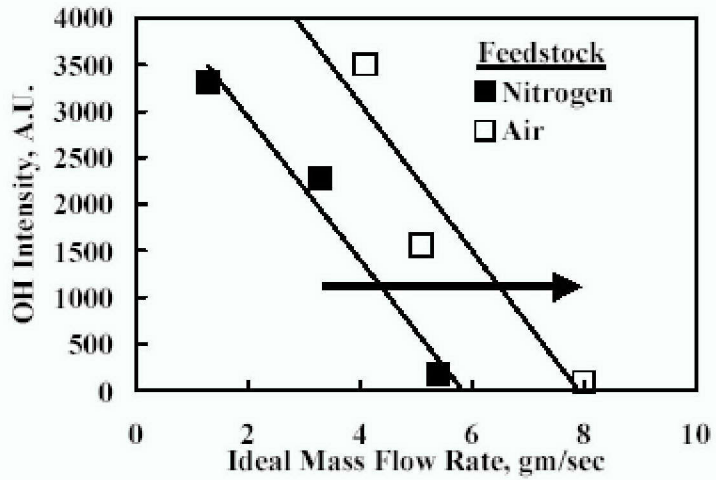

Figure 15. Mean OH intensity 'peak values' for the aero-ramp injector with the VT plasma torch at the second relative downstream torch station and 4KW nominal total input power. Laser sheet was positioned 5.1 cm downstream of the plasma-torch orifice.

Trends of OH signal intensity with varying fuel mass flowrate of VT plasma torch in combination with the aeroramp fuel injector at the second downstream torch location are shown in Figure 15. Notice that the OH level significantly increases for a particular fuel flow rate when air is used as the torch feedstock.

Figure 16 shows a shadowgraph of the VT plasma torch in operation 4.1-cm downstream of the barbotage liquid JP-7/nitrogen injector. In this image the flow is moving from left to right. The dark jet emanating from the bottom left of the image is the due to the barbotaged fuel (i.e., the strong extinction of the schlieren light source due to particle scattering) and the bright light produced on the bottom right-hand side is emission from the interaction of the JP-7 fuel with the VT plasma-torch igniter. Notice that the fuel and plasma jet are within the boundary layer of the wind tunnel floor.

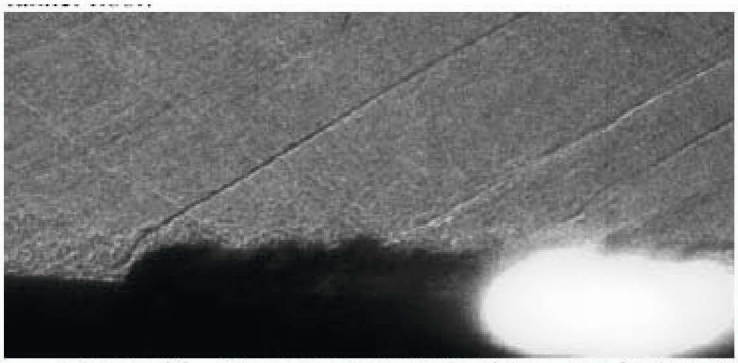

Figure 16. VT plasma torch with a N_2 feedstock downstream of a JP-7/N_2 barbotage injector in a Mach 2 flow (200 ns image). Flow is left to right.

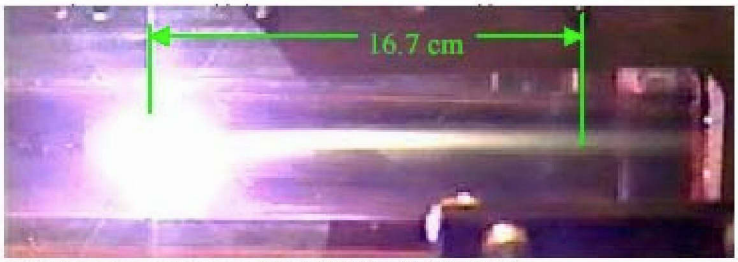

a) Nitrogen plasma jet (4KW, 40 SLPM).

b) Barbotage (JP-7 2.0 gm/sec / N2 25 SLPM), Nitrogen plasma jet (4KW, 40 SLPM).

Figure 17. VT plasma torch with a N_2 feedstock at torch-station #1, just downstream of a JP-7/N_2 barbotage injector in a Mach 2 flow. 16.8 cm from torch to downstream edge of insert.

Still video images of the Barbotage (JP-7/N2) injector with nitrogen plasma from the VT torch are shown in Figure 17. These images show the chemiluminescence plume from the plasma jet (a) in operation alone and (b) with the barbotage injector operating at 2 gm/sec JP-7/25 SLPM N2. In general the flame was not as long as with the gaseous ethylene fuel. It was also found that the JP-7 fuel fluoresced at the same wavelengths being used for the OH measurements. However, the OH LIF signal was typically several times that of the JP-7 at the 2 gm/s fuel flowrate. With increasing fuel flowrate, the OH LIF decreased while that of the fuel increased. From these results it is expected that the barbotaged JP-7 will require a higher input power level from the plasma torch (relative to that seen with ethylene) to achieve a flame that propagates down the length of the combustor. Further testing of this configuration with air plasma and different barbotage gases may

help to enhance the size of the flame. In addition, it is worth mentioning that at the Mach-4 flight condition, the temperatures are ~300 K higher than the value set in this experiment.

An effort to simulate the results from the torch/gaseous ethylene fuel experiments with CFD is also underway. This CFD study incorporates the results from the ambient plasma torch experiments in an effort to refine the boundary conditions which represent the plasma-torch jet. By learning to simulate the combined plasma torch and fuel jet in a supersonic crossflow, it is hoped that a more fundamental understanding of the ignition and flame spreading process will be achieved. With this understanding, further refinement of the ignition process in a full-configuration scramjet combustor will be possible, creating a more robust computational design tool for the simulation of plasma-assisted ignition.

Future Full-Configuration Scramjet-Ignition Experiments

Hot flow trials of the most promising operational configurations will be conducted in a full-scale, continuousflow scramjet combustor direct-connect fixture. The typical test configuration consists of an interchangeable watercooled facility nozzle, water-cooled isolator sections, and a water-cooled fixed geometry combustor. Vitiated air will be supplied to the facility nozzle, providing high-enthalpy conditions for a variety of simulated flight Mach numbers.

These tests will also incorporate a cavity flameholder into the flowpath to study the coupling effects of the fuel/plasma flame plume with the low velocity and high residence times provided from the recirculation zone inside a flush-wall cavity. The proposed combustor has an initial cross sectional dimensions of 10.2 x 3.8 cm and will have a similar configuration to the CFD combustor simulation presented in Figures 2 through 4. It is believed that in order to sustain combustion at Mach 4, a minimum equivalence ratio of about 0.25 will be required, as observed in the experiments by Mathur et al.[17] with ethylene fuel in their slightly larger sized combustor (whose fueling and flameholding configuration was the same as in Figure 2). An estimate of the individual ideal fuel mass flow rate needed to sustain combustion in the proposed four-injector configuration, places the required fuel flowrate – for ethylene or JP-7 – at about 6.7 gm/sec per injector at 900 K and 5.4 atm.

With ethylene fuel at 5.4 gm/sec, the VT plasma torch has established a long flame at nominally 590 K at 4-kW total input power. The full-configuration scramjet-ignition experiments at Mach 4 conditions will attempt to utilize the geometry of the combustor and the cavity flameholder to further propagate this flame throughout the test section. The goal, being: generate enough heat release to separate the wall boundary layers and drive a shock train throughout the combustor, thus achieving global ignition. Past experiments performed by Northam et al.[2] indicate that this is

obtainable with ethylene as the combustor fuel with plasma-torch input-power levels of 2-3 kW. The experiments performed here have also shown that more power (than necessary with ethylene) may be required to obtain ignition in a JP-7 fueled engine, as is also suggested by the experiments performed by Northam et al.[2] with methane as the combustor fuel.

Defining Constraints

The initial constraints for concept comparison and evaluation are defined by energy input and igniter size. As the process continues, more overall systems-type constraints may be introduced based on igniter success. Initially the combustor inlet Mach number will be in the range of 1.8 to 2.2, depending on the facility, in order to simulate flight Mach numbers in the range of 4 to 5.

The energy constraints of the plasma ignition devices are defined by short pulse (ignition) and a steady state (flame-holding) operation. The CFD simulations show the development of a minimum ignition-time constraint on the order of a few milliseconds. Due to the short duration of the ignition period thought to be required, no torch energy constraint is currently enforced. However, overall system size may, in the future place a cap on the energy available. Steady-state operation of a device is currently limited to below 10-kW total input power per port with a desired goal of less than 2 kW.

The constraint on igniter size is based on the physical access to the test hardware. This leaves a maximum of 3.8 cm of space between the igniters in an injector-coupled design in the full engine configuration of AFRL/PRA Test Cell 22. Currently, a torch design with a 2.3-cm diameter or less is sought to mitigate hardware integration difficulties in the new combustor being developed in AFRL/PRA Test Cell 18, which has a 2.5-cm spacing between its proposed lateral array of four fuel injectors.

Conclusions

The main goal of the Air Force plasma ignition program is to asses the prospect of main fuel ignition with plasma generating devices in a supersonic flow. As the study progresses, baseline conditions of operation are being established – such as the required operational time of the device to initiate a combustion shock train. Computations suggest that the average power required for ignition is within reasonable limits.

The torches in use at this time show two different ways of introducing energy in the form of plasma into a fueled, supersonic crossflow. Not only do they differ in the type of power used to produce their plasma (DC and AC), they also differ substantially in orifice geometry and thus the range of feedstock mass flowrate. In addition, the plasma torches are realistic in size and operate within current power constraints.

In order to compare the potential of each concept, an understanding of the flow physics of each part of the system – separate and together – is being achieved. Coupled between CFD and experiment, each step of the program is taking advantage of the benefits of both methods to help understand and advance the ignition process.

To understand the constraints involved with ignition process of a hydrocarbon fuel jet, an experimental effort to study gaseous and liquid hydrocarbons is underway, involving the testing of ethylene and JP-7 fuels with nitrogen and air plasmas. Results from the individual igniter studies have shown the plasma igniters to produce hot pockets of highly excited gas with peak temperatures above 5000 K at only 2-kW total input power. In addition, ethylene and JP-7 fueled flames were also produced in a Mach-2 supersonic flow with a total temperature and pressure of 590 K and 5.4 atm, respectively.

As the constraints involved with the ignition process are further understood, this in turn will help evolve the design and use of the igniters investigated. Finally, with the success of this program, an alternative to existing starting methods, such as silane or a gas generator, will be established which is non-toxic, multi-use, and capable of being integrated into the next generation of hydrocarbonfueled scramjet applications.

Acknowledgements

This work has been supported by the Air Force Office of Scientific Research (AFOSR) and the Nunn Program Office. We would also like to thank the following people for their contributions to the plasma-assisted ignition effort at the AFRL: Joseph Schetz and Walter O'Brien of Virginia Tech, Spencer Kuo and Daniel Bivolaru of Polytechnic University, Greg Elliot and Martin Boguzko of Rutgers University, Jim Crafton and Mark Hsu of Innovative Scientific Solutions, Inc., P.-K. (Steven) Lin, Paul Kennedy, Bill Terry, Dave Schomer, and Gary Streby of Taitech, Inc., and Skip Williams of the AFRL/VS.

References

1. Kimura, I., Aoki, H., and Kato, M., "The Use of a Plasma Jet for Flame Stabilization and Promotion of Combustion in Supersonic Air Flows," *Combustion and Flame*, Vol. 42, pp. 297-305, 1981.

2. Northam, G., McClinton, C., Wagner, T., and O'Brien, W., "Development and Evaluation of a Plasma Jet Flameholder for Scramjets," AIAA Paper 84-1408, June 1984.

3. Wagner, T., O'Brien, W., Northam, G., and Eggers, J., "Plasma Torch Igniter For Scramjets," *Journal of Propulsion and Power*, Vol. 5, No. 5, 1989.

4. Kanda, T., Hiraiwa, T., Mitani, T., Tomioka, S., and Chinzei, N., "Mach 6 Texting of a Scramjet Engine Model," *Journal of Propulsion and Power*, Vol.13, No. 4, 1997.

5. Fuji, S., Shuzenji, K., Kato, R., and Tachibana, T, "Augmentation of Ignition Arcs for Air Breathing Combustion by Teflon Sublimates," AIAA Paper 1998-3215, July 1998.

6. L. S. Jacobsen, S. D. Gallimore, J. A. Schetz, and W. F. O'Brien, "An Integrated Aeroramp Injector / Plasma-Igniter for Hydrocarbon Fuels in a Supersonic Flow. Part A: Experimental Studies of the Geometrical Configuration," AIAA Paper 2001-1766, April 2001.

7. S. D. Gallimore, L. S. Jacobsen, W. F. O'Brien, and J. A. Schetz, "An Integrated Aeroramp Injector / Plasma-Igniter for Hydrocarbon Fuels in a Supersonic Flow. Part B: Experimental Studies of the Operating Conditions," AIAA Paper 2001-1767, April 2001.

8. Williams, S., Arnold, S., Bench, P., Viggano, A., Dotan, I., Midey, A., Morris, T., Morris, R., Maurice, L., and Sutton, E., "Potential Enhancement of Hydrocarbon Fueled Combustor Performance Via Ionization", ISABE Paper 99-7236, 1999.

9. Sato, Y., Sayama, M., Ohwaki, K., Masuya, G., Komuro, T., Kudou, K., Murakami, A., Tani, K, Wakamatsu, Y., Kanda, T, Chinzei, N., Kimura, I., "Effectiveness of Plasma Torches for Ignition and Flameholding in Scramjet," AIAA Paper 89-2564, July 1989.

10. Masuya, G., Kudou, K., Komuro, T., Tani, K., Kanda, T., Wakamatsu, Y., Chinzei, N., Sayama, M., Ohwaki, K., and Kimura, I., "Some Governing Parameters of Plasma Torch Igniter/Flameholder in a Scramjet Combustor," *Journal of Propulsion and Power*, Vol. 9, No. 2, pp. 176-181, 1993.

11. Tomioka, S., Hiraiwa, T., Sakuranaka, N., Murakami, A., Sato, K., and Matsui, A., "Ignition Strategy in a Model Scramjet," AIAA Paper 96-3240, July 1996.

12. Masuya, G., Takita, K., Sato, T., Ohwaki, K., Takahashi, K., Uemoto, T., Ju, Y., and Matsumoto, M., "Ignition of Parallel and Low Angle Hydrogen Jet by Plasma Torch," 14th ISABE Conference, September 1999.

13. Kobayashi, K., Tomioka, S., and Mitani, T., "Ignition by an H_2/O_2-Microburner in a Supersonic Flow," AIAA Paper 2001-1763, April 2001.

14. Shuzenji, K., Kato, R., and Tachibana, T., "Two-Stage Plasma Torch Ignition in Supersonic Airflows," AIAA Paper 2001-3740, July 2001.

15. Masuya, G., Choi, B., Ichikawa, N., and Takita, K., "Mixing and Combustion of Fuel Jet in Pseudo-Shock Waves," AIAA Paper 2002-0809, January 2002.

16. Pandolfini P. P., Billig, F. S., Corpening, G. P., Corda, S., and Friedman, M., A., "Analyzing Hypersonic Engines Using the Ramjet Performance Analysis Code," *APL Technical Review*, Vol. 2, No. 1, 1990, pp 68-79.

17. Mathur, T., Streby, G., Gruber, M., Jackson, K., Donbar, J., Donaldson, W., Jackson, T., Smith, C., and Billig, F., "Supersonic Combustion Experiments with a Cavity-Based Fuel Injector," AIAA Paper 99-2102, June 1999.

18. White, J. A. and Morisson, J. H., "Pseudo-Temporal Multi-Grid Relaxation Scheme for Solving the Parabolized Navier-Stokes Equations," AIAA Paper 99-3360, June 1999.

19. Edwards, J. R., "A Low Diffusion Flux-Splitting Scheme for Navier-Stokes Calculations," Computers & Fluids, Vol. 26, pp. 635-659, No. 6, 1997.

20. Baurle, R. A., Mathur, T., Gruber, M. R., and Jackson, K.R., "A Numerical and Experimental Investigation of a Scramjet Combustor for Hypersonic Missile Applications," AIAA Paper 98-3121, July 1998.

21. Jacobsen, L. S., Carter, C. D., Jackson, T. A., Schetz, J.A., O’Brien, W. F., G. S. Elliott, M. Boguzko, and J. W. Crafton "An Experimental Investigation of a DC Plasma-Torch Igniter," AIAA Paper 2002-5228, September 2002.

22. Kou, S. P., Koretzky, E., and Orlick, L., "Design and Electrical Characteristics of a Modular Plasma Torch," IEEE Trans. Plasma Sci. Vol. 27, No. 3, pp. 752-758 , 1999.

23. Behbahani, H., Fontijn, A., Mueller-Dethlefs, K., and Weinberg, F., "The destruction of Nitric Oxide by Nitrogen Atoms from Plasma Jets," *Combustion Science and Technology*, Vol. 27, 1982, pp. 123-132.

24. Jacobsen, L. J., Gallimore, S. D., Schetz, J. A., and O’Brien, W. F., "An Improved Aerodynamic Ramp Injector in Supersonic Flow," AIAA Paper 2001-0518, January 2001.